Development of calcium stabilized nitrogen rich alpha-sialon ceramics along the Si3N4:1/2Ca3N2:3AlN line using spark plasma sintering

Bilal Anjum Ahmed
National Kaohsiung University of Science and Technology
Abbas Saeed Hakeem
King Fahd University of Petroleum & Minerals
Tahar Laoui (tlaoui@hotmail.com)
University of Sharjah https://orcid.org/0000-0002-9527-6610

Research Article

Keywords: Nitrogen rich sialon ceramics, Alpha sialon, Calcium sialons, Spark plasma sintering, Liquid phase sintering

Posted Date: June 12th, 2020

DOI: https://doi.org/10.21203/rs.3.rs-21600/v2

Abstract

Calcium stabilized nitrogen rich sialon ceramics having a general formula of $Ca_xSi_{12-2x}Al_{2x}N_{16}$ with x value in the range of 0.2-2.2 for compositions lying along the Si_3N_4:1/2Ca_3N_2:3AlN line were synthesized using nano/submicron size starting powder precursors and spark plasma sintering (SPS) technique. The development of calcium stabilized nitrogen rich sialon ceramics at a significantly low sintering temperature of 1500°C (typically reported a temperature of 1700°C or greater) remains to be the highlight of the present study. The SPS processed sialons were characterized for their microstructure, phase and compositional analysis, physical and mechanical properties. Furthermore, a correlation was developed between the lattice parameters and the content (x) of the alkaline metal cation in the alpha-sialon phase. Well densified single-phase nitrogen rich alpha-sialon ceramics were achieved in the range of $0.53(3) \leq x \leq 1.27(3)$. A nitrogen rich alpha-sialon sample possessing a maximum hardness of 22.4 GPa and fracture toughness of 6.1 $MPa.m^{1/2}$ was developed.

1. Introduction

Sialon materials is a class of ceramics that have been thoroughly studied with respect to their phase stability regimes, thermo-mechanical properties, photoluminescence and oxidation behavior [1–11]. Most of the work on sialon ceramics has been concentrated around the two commonly known phases, namely alpha-sialon and beta-sialon. A compound of silicon nitride, beta-sialon having a general formula of $Si_{6-z}Al_zO_zN_{8-z}$, is formed as a result of the chemical replacement of silicon-nitrogen bonds with aluminum-oxygen bonds[12].

Compositions belonging to alpha-sialon phase are generally defined by $M_x^vSi_{12-(m+n)}Al_{m+n}O_nN_{16-n}$ (x and v represent solubility and valence of the cation M in alpha-sialon structure, respectively) where x < 2, x = mv, and m (Al-N) and n (Al-O) replace (m+n) (Si-N) bonds[13]. The substitution of silicon-nitrogen bonds with aluminum-nitrogen and aluminum-oxygen bonds results in a charge imbalance which is neutralized by the incorporation of M^{v+} ions such as Li^+, Ca^{2+}, Mg^{2+}, Y^{3+} and lanthanide ions [14–17]. Studies have been reported on synthesis and phase stability regime of single phase alpha sialons [14–19]. Several compositions of yttrium-stabilized alpha-sialons along the nitrogen rich line of Si_3N_4–YN:3AlN were synthesized by Sun et al. where the solubility limit of yttrium cation in alpha sialon was found out to be 0.43<x<0.8 [1]. Zhen-Kun et al. studied the formation of oxygen rich yttrium stabilized alpha-sialons along the Si_3N_4–Y_2O_3:9AlN and the solubility limit of yttrium cations was reported as 0.33<x<0.67 [14]. It is well known that synthesis of alpha-sialons occurs via a solution-reprecipitation mechanism, which involves the formation of an intermediary oxy-nitride liquid phase as a result of the reaction between the starting oxide and nitride precursors [20,21].

In contrast to alpha-sialons synthesized using yttrium or rare earth stabilizing cations, calcium stabilized alpha-sialons have gained considerable attention due to the higher solubility of calcium cation as compared to the former (maximum solubility value x_{max} of 1.6 for Ca^{+2} as compared to x_{max} value of 1.0

for Yb^{+2}) [15,17]. Furthermore, Hassan Mandal, in his study on post sintering heat treatment of alpha sialons, reported that in contrast to rare-earth stabilized alpha-sialons, calcium stabilized alpha-sialons depicted complete resistance towards alpha to beta phase transformation in the temperature range of 1450-1500°C [22].

The higher stability of calcium stabilized alpha-sialons has been attributed to the lower valency of calcium cation, since the high temperature stability of alpha-sialon increases with increase in the solubility of charge stabilizing cation (x), which in turn increases with decrease in cation valency [23].

Figure 1 shows the Janecke prism and the calcium alpha-sialon plane highlighting the single-phase alpha-sialon region (oxygen rich as well as nitrogen rich) along with the neighboring phases at 1800°C [24]. Several studies conducted on the synthesis of oxygen rich alpha-sialons have reported the formation of elongated morphology of alpha-sialon as compared to the generally known equiaxed morphology, thus resulting in considerable improvement in the toughness of these materials [25–27]. However, there are very few studies that have been reported on the synthesis of nitrogen-rich alpha-sialons, mainly due to the fact that they are difficult to densify [23,28]. Studies on the synthesis of calcium stabilized nitrogen rich alpha-sialons using all nitride precursors is even more scarce in the literature due to the difficulty in handling and storage of calcium nitride [23].

Xie et al. worked on the synthesis of calcium stabilized nitrogen rich alpha-sialons along the Si_3N_4-$1/2Ca_3N_2$:3AlN line at 1700°C using hot pressing technique [23]. The limits of single phase calcium alpha-sialon was reported to be $0.5<x<1.7$. Later, Yanbing Cai et al. studied the synthesis of calcium stabilized nitrogen rich alpha-sialons using CaH_2 as a starting precursor instead of Ca_3N_2 at 1800°C using hot pressing (HP) technique [28]. Single phase alpha sialon ceramics were obtained in the range of $0.50<x<1.38$. Densification using conventional sintering processes, such as hot press (HP), is governed by the heat supplied via heating elements (comparatively much slower heating rate than SPS) and the externally applied pressure [29].

On the other hand, for the non-conventional and modern sintering process spark plasma sintering (SPS), in addition to the uniaxial applied pressure, the pulsed nature of the current creates spark discharge and gives rise to joule heating effect between the powder particles. The high rate of plasma discharge transmits and distributes the Joule heat throughout the material. This phenomenon results in a fast and uniform heat distribution within the sample, which ultimately leads to highly homogeneous samples with consistent densities. In addition, the high heating/cooling rate is beneficial as it restricts the grain growth as well as the formation of intermediate phase(s). Samples can be densified in very short time by SPS [29,30]. Raja et al. has reported the synthesis of oxygen rich calcium alpha-sialon ceramics at relatively low temperature of 1500°C using nano-sized precursors and SPS technique [31]. However, to our knowledge, synthesis of nitrogen rich sialons at low temperatures (below 1700°C) has not been reported in the literature.

The aim of the present study was to develop calcium stabilized nitrogen rich alpha-sialons along the Si_3N_4:1/2Ca_3N_2:3AlN line at a relatively low temperature of 1500°C using SPS and nano-/submicron-size starting powder precursors. The developed sialons were characterized for their microstructure, phase and compositional analysis, physical and mechanical properties. Furthermore, a correlation was developed between the lattice parameters and the content of alkaline metal cation (calcium) in the alpha-sialon.

2. Experimental Procedure

Calcium stabilized nitrogen rich alpha-sialon compositions having the general formula of $Ca_xSi_{12-m}Al_mN_{16}$ (where x = m/2), along the nitrogen rich line, were selected in this study. The nominal x value varied in the range of 0.2-2.2. Actually achievable compositions of alpha-sialon samples (by taking into account the oxide content on the powder surface) as listed in **Table 1** were synthesized using starting powder precursors of alpha-Si_3N_4 with an average particle size of ~300 nm (Ube Industries SN-10, Japan), AlN with the particle size of ~50nm (ChemPUR, Germany) and Ca_3N_2 of ~74µm (~200 mesh, Sigma Aldrich, Germany). The oxygen content in the Si_3N_4, AlN and Ca_3N_2 powders corresponds to 2.87 wt% SiO_2, 1.75 wt% Al_2O_3 and 3.5 wt% CaO, respectively. The sample ID's used in this manuscript starts with the letter 'Ca' followed by the nominal value of 'x' selected for the synthesis of a specific composition. For example, a sample having the chemical formula of $\mathbf{Ca_{0.2}Si_{11.6}Al_{0.4}O_{0.52}N_{15.31}}$ is referred to as Ca-0.2. Since Ca_3N_2 is very sensitive to moisture and air and quickly decomposes into calcium hydroxide and ammonia, powders of silicon nitride and aluminum nitride (required to synthesize 5 gm of a specific composition) were initially mixed via ultrasonic-probe sonicator in ethanol medium. The sonicated powder mixture was then dried in oven at 95°C for a period of 24h to evaporate ethanol. The dried powder mixture of silicon nitride and aluminum nitride was then mixed with the required amount of calcium nitride using mortar and pestle in NEXUS II glove box (Vacuum Atmosphere Company, USA) under the presence of high purity argon gas. The powder mixture thoroughly mixed for about 15-20 minutes was then poured into a 20mm graphite die lined with BN, and the die was sealed with parafilm. The sealed die was taken out of the glove box and placed within the SPS chamber. The powder mixtures were synthesized (compacted and sintered) using an SPS apparatus (FCT system, model HP D5, Germany), calibrated and maintained by the manufacturer, on a yearly basis. The schematic of the SPS machine is shown in **figure 2**. During the synthesis process, the temperature was monitored and controlled using a pyrometer, fixed just above the upper punch, measuring the temperature only 3 mm away from the top surface of powder mixture inside the graphite die. Moreover, as shown in the schematic, the temperature of the die was also measured using a K-type thermocouple, placed in the center of the die, only 3 mm away from the powder sample in the die. The maximum temperature difference of less than ±20°C, measured between pyrometer and thermocouple, assured the in-depth calibration.

The powder mixture was consolidated into 20mm diameter pellets at a sintering temperature of 1500°C with 30 minutes holding time in a vacuum environment and 50MPa of constant uniaxial pressure. The heating rate of 100°C/min was used in the synthesis, followed by constant temperature holding process, then samples were cooled down to room temperature within 5 minutes. Each sample was prepared twice and densification data was obtained from the SPS equipment. The shrinkage curves were generated using the experimental data (relative piston displacement, time and temperature values) collected and stored automatically on the FCT SPS software. The synthesized samples were cleaned of graphite using SiC grinding paper and were further ground and polished using Automet 300 Buehler grinding machine to a surface finish of 1µm. Phase analysis was performed using Bruker D8 X-ray powder diffractometer with Cu $K_{\alpha 1}$ radiation (γ = 0.15416 nm). The tube current of 40mA, accelerating voltage of 40 kV, step size of 0.02 degrees and step time of 3sec were maintained during the entire scan. In order to calculate the lattice parameters of alpha-sialon accurately, silicon powder was used as an internal standard. The amount of alpha and beta phases was calculated using the following equation [32]: (see Equation 1 in the Supplemental Files)

Where I_{α} represent observed intensities of (102) and (210) peaks belonging to alpha-phase while I_{β} represents observed intensities of (101) and (210) peaks belonging to beta-phase. W_{β} represents fraction of beta-phase while K is the proportionality constant (0.518 for β(101) and α(102) peaks while 0.544 for β(210) and α(210) peaks [32]. The amount of minor phases was determined based on the relative intensity method. Highly polished and fractured surfaces of the synthesized samples were observed using a field emission scanning electron microscope (FESEM, Lyra3, Tescan, Czech Republic) with an accelerating voltage of 20 kV. Phoenix focused ion beam (Helios G4 UX DualBeam, FEI) was used to prepare the lamellas for observation under a transmission electron microscope (TEM). High resolution imaging and selected area diffraction patterns were acquired using FEI's Titan transmission electron microscope equipped with EDX detector. On average, five area EDX analyses were performed to calculate the cation composition. The software UnitCellWin and XRD peak positions were used to calculate the lattice parameters. The density of the synthesized disk shaped samples (after removal of graphite) was calculated using Archimedes' principle. Vickers hardness (HV_{10}) was measured on the surface of the polished samples using a universal hardness tester (Zwick-Roell, ZHU250, Germany). The indentation load of 10kg was adopted for the hardness test. Indentation method was used to calculate the fracture toughness (K_{1c}) of the synthesized samples [33–36]. Evan's equation shown below was used to calculate the indentation fracture toughness. In the equation 'MCL' stands for the maximum crack length initiated from the indentation and 'd' is the average diagonal: (see Equation 2 in the Supplemental Files)

Table 1 Starting composition of calcium stabilized nitrogen rich sialons, along with sample ID, mole composition and weight ratio are shown in the table.

*Actually achievable compositions calculated by taking into account the oxide content in the starting powder precursors.

3. Results And Discussion

Sample ID	Starting Composition*	Ca_3N_2 wt%	Si_3N_4 wt%	AlN wt%
Ca-0.2	$Ca_{0.2}Si_{11.6}Al_{0.4}O_{0.52}N_{15.31}$	1.74	95.37	2.89
Ca-0.4	$Ca_{0.4}Si_{11.2}Al_{0.8}O_{0.52}N_{15.32}$	3.43	90.87	5.70
Ca-0.6	$Ca_{0.6}Si_{10.8}Al_{1.2}O_{0.52}N_{15.34}$	5.08	86.48	8.44
Ca-0.8	$Ca_{0.8}Si_{10.4}Al_{1.6}O_{0.52}N_{15.35}$	6.68	82.20	11.11
Ca-1.0	$Ca_{1.0}Si_{10}Al_{2.0}O_{0.51}N_{15.36}$	8.25	78.04	13.71
Ca-1.2	$Ca_{1.2}Si_{9.6}Al_{2.4}O_{0.51}N_{15.38}$	9.78	73.98	16.25
Ca-1.4	$Ca_{1.4}Si_{9.2}Al_{2.8}O_{0.51}N_{15.39}$	11.26	70.02	18.72
Ca-1.6	$Ca_{1.6}Si_{8.8}Al_{3.2}O_{0.50}N_{15.40}$	12.71	66.15	21.13
Ca-1.8	$Ca_{1.8}Si_{8.4}Al_{3.6}O_{0.50}N_{15.42}$	14.13	62.38	23.49
Ca-2.0	$Ca_{2.0}Si_{8.1}Al_{3.9}O_{0.50}N_{15.43}$	15.51	58.70	25.79
Ca-2.2	$Ca_{2.2}Si_{7.7}Al_{4.3}O_{0.50}N_{15.44}$	16.86	55.11	28.03

3.1 Synthesis and Densification Behavior

Densification behavior of the samples synthesized over the range of 0.2<x<2.2 is shown in **figure 3** (inserted figure shows the complete densification curves), where the ordinate represents the displacement of an upper punch of the die in mm, depicting the shrinkage, while the abscissa represents the synthesis/sintering time. It is observed that with the increase in the x value, denoting the increase in calcium (Ca) content, the shrinkage curve shifts to the left (towards shorter time). Samples having higher x value exhibit a more significant shrinkage (larger displacement) and subsequently are more densified than at the earlier stage of synthesis. It is quite known that the densification of silicon nitride based materials involve the formation of a transient liquid phase, where the densification behavior depends on the viscosity; amount and wetting characteristic of the transient liquid phase. In case of the calcium stabilized alpha-sialons synthesized using oxide additives, the formation of transient liquid phase takes place as a result of the reaction between silicon oxide present on the surface of silicon nitride powder and oxide additives. In our case, there are basically two sources of a liquid phase. Firstly, due to the eutectic reaction between silicon oxide, aluminum oxide and calcium oxide present on the surfaces of starting nitride precursors, and secondly due to the melting of calcium nitride which takes places at about 1195°C (since calcium nitride is not used as a starting precursor in the synthesis of oxygen rich calcium alpha-sialons) [37]. Furthermore, since the oxide rich eutectic liquid phase is produced as a result of the surface oxide layer present on the surface of starting nitride precursors, the amount of oxide rich transient liquid is very small. On the other hand, the amount of nitrogen liquid phase formed because of melting of calcium nitride increases, with the increase in x value (more calcium nitride) and consequently resulted in easier densification (higher shrinkage within a shorter time) of the samples having high x value. Xie et al. reported a similar trend for the nitrogen rich alpha-sialons synthesized using HP technique and micron size precursors at 1700°C and 1h holding time [23]. However, the reported shrinkage rate was much slower due to the slower reaction kinetics as a result of the conventional heating technique (slower heating rate) as well as due to larger size (>1μm) of the starting powder precursors.

Table 2 shows the density values of the nitrogen rich calcium stabilized alpha-sialons for compositions having x values in the range of 0.2-2.2, synthesized at a relatively low temperature of 1500°C. The density of the samples synthesized at 1500°C was measured to be in the range of 2.96-3.21 g/cm^3 and was seen to increase with the increase in x value (increase in Ca_3N_2 content). Xie et al. reported comparable density values (3.10-3.15 g/cm^3) with a similar trend for the nitrogen rich alpha-sialons

synthesized at 1700°C using HP technique and micron size precursors [23]. Yanbing Cai et al. worked on the synthesis of calcium stabilized nitrogen rich alpha-sialons at 1800°C using HP technique [28]. The observed density values were reported to be in the range of 3.16-3.26 g/cm^3. Furthermore, Wang et al. reported density values of 3.07g/cm^3 and 3.17g/cm^3 at 1700°C and 1750°C, respectively, for dense hot-pressed oxygen rich calcium alpha-sialon having a composition of $Ca_{0.5}Si_{10.5}Al_{1.5}O_{0.5}N_{15.5}$ [38]. Xie et al. communicated a failure to synthesize well densified yttrium stabilized nitrogen rich alpha-sialons along the Si_3N_4:YN:3AlN where an insufficient amount of liquid phase was provided to be the main reason [23]. This suggests that along with nano-size starting precursors and novel pulsed-based SPS technique, low melting temperature (1195°C) of calcium nitride plays a pivotal role in achieving well densified samples at 1500°C. This is in line with the literature where it has been reported that a small particle size of starting powders helps to synthesize dense sialon materials at low temperatures [39,40].

Table 2 Density of calcium stabilized nitrogen rich alpha-sialon sintered at 1500°C.

Sample ID	Ca-0.2	Ca-0.4	Ca-0.6	Ca-0.8	Ca-1.0	Ca-1.2	Ca-1.4	Ca-1.6	Ca-1.8	Ca-2.0	Ca-2.2
c	0.2	0.4	0.6	0.8	1	1.2	1.4	1.6	1.8	2	2.2
Density (g/cm^3)	2.96	3.06	3.09	3.14	3.17	3.17	3.18	3.19	3.20	3.20	3.21

3.2 Phase Analysis

Figure 4 shows X-ray diffraction patterns of the samples synthesized at 1500°C. Single phase calcium stabilized alpha-sialon phase is observed for samples produced in the range of $0.6 \leq x \leq 1.4$ (Ca-0.6 to Ca-1.4). Dual phases (alpha and beta-sialons) are observed for samples having $x \leq 0.4$, where the amount of beta-sialon phase is seen to decrease as the composition shifts towards single phase alpha-sialon. Beyond the single-phase region, alpha-sialon coexists with AlN and $CaSiAlN_3$ in the range of $1.6 \leq x \leq 2.0$. **Figure 5a** displays the regenerated schematic representation of α-plane in Ca-sialon system showing phase stability regime region along the N'Rich line at 1500°C where **figure 5b** represents the same, where the orientation of the alpha plane is the one which is most commonly presented in the literature. A similar observation is reported by Xie et al. for the calcium stabilized nitrogen rich samples synthesized at 1700°C using HP technique [23]. Furthermore, Yabaing et al. in their work on the synthesis of nitrogen rich sialons at 1800°C, have also communicated the formation of AlN and $CaSiAlN_3$ phases along with alpha-phase for higher values of x (x>1.6) and the single phase alpha-sialon phase is reported to be in the range of $0.6 \leq x \leq 1.6$ [24].

X-ray diffraction results of the samples synthesized at 1500°C are summarized in **Table 3**. Lattice parameters of alpha sialon are seen to increase with the increase in x value attributed to the fact that more amount of Si-N bonds are replaced by Al-N bonds as well as more amount of calcium ion is being incorporated in the structure. In calcium stabilized alpha-sialons, the charge imbalance caused as a result of the substitution of Si^{+4} for Al^{+3} is brought into balance by the addition of Ca^{+2} ions at the interstitial

positions in the network. It is established that alpha-sialon unit cell contains two interstices per unit cell, the upper solubility limit of calcium ion(s) in alpha-sialon having a composition of $Ca_2Si_8Al_2N_{16}$ is ideally believed to be 2. However, due to the unavoidable presence of the oxide layer on the surface of starting precursors, this composition has not been achieved so far. Yabing et al. in their work on the synthesis of nitrogen rich sialons at 1800°C, have reported a maximum achieved solubility limit of 1.82 for nominal x value of 2.2 [28]. Similarly, Xie et al. reported the maximum solubility value of 1.7 for the calcium stabilized nitrogen rich samples synthesized at 1700°C using HP technique [23]. In our case, the maximum solubility limit has been determined to be 1.83 for the nominal x value of 2.2.

Table 3 Lattice parameters, mechanical properties and phase assemblage of calcium stabilized nitrogen rich sialons synthesized at 1500°C.

Sample ID	c(Ca)		Lattice Parameters		HV_{10}	K_{1c}	Phase Assemblage
	Nom	EDXS	a(Å)	c(Å)	GPa	$MPa.m^{1/2}$	wt%
Si_3N_4*	0	-	7.7541	5.6217	-	-	-
Ca-0.2	0.2	0.15(2)	7.7814(6)	5.6490(4)	18.5 (3)	4.5 (4)	α (61), β (39)
Ca-0.4	0.4	0.33(3)	7.7971(6)	5.6593(4)	19.4 (7)	5.0 (4)	α (87), β (13)
Ca-0.6	0.6	0.53(3)	7.8210(7)	5.6631(5)	22.2 (2)	5.6 (3)	α (100)
Ca-0.8	0.8	0.73(3)	7.8343(7)	5.6885(5)	22.4 (5)	5.7 (3)	α (100)
Ca-1.0	1.0	0.84(4)	7.8470(7)	5.7011(5)	21.8 (4)	5.7 (3)	α (100)
Ca-1.2	1.2	1.01(5)	7.8770(7)	5.7153(4)	21.6 (2)	5.3 (2)	α (100)
Ca-1.4	1.4	1.27(3)	7.8937(7)	5.7316(5)	21.0 (3)	6.1 (3)	α (100)
Ca-1.6	1.6	1.39(4)	7.9170(7)	5.7464(5)	20.8 (4)	5.8 (2)	α (82), A (10), C (8)
Ca-1.8	1.8	1.54(5)	7.9320(6)	5.7583(5)	20.1 (7)	5.5 (3)	α (82), A (9), C (9)
Ca-2.0	2.0	1.68(4)	7.9534(7)	5.7695(5)	19.3 (6)	5.7 (2)	α (79), A (10), C (11)
Ca-2.2	2.2	1.83(5)	7.9651(6)	5.7790(4)	18.7 (5)	5.2 (3)	α (75), A (12), C(13)

*JCPDS 41-0360, (Nom) Nominal, (α) Alpha Sialon, (β) Beta-Sialon, (A) Aluminum Nitride (JCPDS 25-1133), (C) $CaSiAlN_3$ (JCPDS 39-747).

Figure 6 shows the variation of alpha sialon lattice parameters with respect to change in x value. Similar behavior is reported by Yabning for samples synthesized at 1800□C (figure 6) [24]. The dependence of alpha-sialon lattice parameters with the amount of Ca+2 can be well defined by the following empirical relationships:

$a = 0.0949x + 7.7605$ (Å) (1)

$c = 0.0680x + 5.6326$ (Å) (2)

Formation of alpha-sialon phase for a sample having x value as low as 0.2 along with the observation suggesting a linear dependence of alpha-sialon unit cell parameters with x value, provide a good reason to believe that calcium stabilized nitrogen rich alpha-sialon forms continuously in the range of $0<x<1.83$. Therefore, the previously reported low solubility limit of Ca^{+2} in alpha-sialons shall not be attributed to a

structural limitation but should rather be ascribed to the fact that formation of single phase alpha-sialons near the nitrogen rich corner has not been attained due to the presence of the oxide layer contamination leading to the formation of beta-sialon phase.

3.3 Microstructure Analysis

Figure 7 (a-f) depicts the secondary electron FESEM micrographs of the fractured surface of samples from the nitrogen rich sialon ceramics sintered at 1500°C. Primarily, a classical intergranular fracture was observed in all samples, along with some amount of grain pullout. Sample Ca-0.2 containing alpha- and beta-sialon phases exhibit elongated morphology of beta-sialon along with smaller equiaxed grains of alpha-sialon (**figure 7a**). Samples with x values greater than 0.4 (Ca-0.6 to Ca-2.2) composed of single phase or almost single-phase nitrogen rich calcium alpha-sialon depicted fine equiaxed grains (a morphology typical of alpha-sialon phase). However, with the increase in x value (more Ca_3N_2), alpha-sialon grains with elongated morphology are also observed. Additionally, it is observed that an increase in x value yields an increase in the average grain size of alpha-sialon. The grain size distribution for the three samples (Ca-0.6, Ca-1.2 and Ca-2.0) is depicted in **figure 8** where the average grain size is measured to increase from 286 $\pm$98nm to 385 $\pm$96nm to 468$\pm$169 nm respectively.

Figure 9 (a-e) shows the low and high resolution TEM images of the microstructures of nitrogen rich calcium alpha-sialon samples (having the ID's as Ca-0.6, Ca-1.2 and Ca-2.0). In accordance with the observations made on fractured surfaces, sample Ca-0.6 displays an equiaxed morphology of alpha-sialon grains with an average grain size of 277 $\pm$34.56nm. For samples Ca-1.2 and Ca-2.0, a dual morphology of alpha-sialon grains, i.e. elongated grains alongside the equiaxed grains, is observed. The average size of the grains is measured to be 386 $\pm$127nm for Ca-1.2 and 449 $\pm$142nm for Ca-2.0. Alpha-sialon ceramics having an elongated morphology as a result of preferential grain growth during the densification process has also been reported in the synthesis of hot-pressed oxygen rich Ca-alpha-sialons [11,38,41]. It is known that the grain growth of alpha-sialon takes place via solution, re-precipitation mechanism and that the presence of a liquid phase is necessary to promote grain growth. Therefore, the presence of elongated morphology of alpha-sialon grains as well as the grain growth for samples having higher x value (i.e. more Ca_3N_2) may well be attributed to the formation of a higher amount of transient liquid phase. Thorel et al. in their study on high temperature mechanical properties and intergranular structure of sialons (oxygen rich) have reported that intergranular phase (if present) is always amorphous and can exist as reasonably large pockets having a size in the range of 0.1 to 1µm or interfacial glassy film with a minimum reported thickness of about 60nm [42]. In our study, the high-resolution TEM images of nitrogen rich sialons (**figure 9 b, d, and e**) reveal that there is no sign of a glassy phase present at the grain boundaries nor at the junction of multiple grains. These results suggest that the synthesized nitrogen rich sialons would be more stable at high temperature (1400-1600°C) compared to the oxygen rich sialons containing an amorphous phase on the grain boundaries.

3.4 Mechanical Properties

Vickers hardness (HV_{10}) and fracture toughness (K_{1c}) of the calcium stabilized nitrogen rich alpha-sialons synthesized at 1500°C are summarized in Table 3. The two-phase sample (Ca-0.2), having alpha- and beta-sialon phases, displays a hardness of 18.5 GPa and fracture toughness of 4.5 MPa.$m^{1/2}$. The Vickers hardness of the single-phase alpha-sialon samples (Ca-0.6 – Ca-1.4) are found to be in the range of 21.0-22.4 GPa while the fracture toughness is measured to be in the range of 5.6-6.1 MPa.$m^{1/2}$. Presence of elongated morphology of alpha-sialon grains for samples having higher x value (i.e. more Ca_3N_2) may well be attributed to the formation of a higher amount of transient liquid phase. With not much of a difference, the highest fracture toughness of the sample Ca-1.6 is attributed to the relatively elongated morphology of α-Sialon. For samples having x value greater than 1.6, a gradual decrease in the hardness is observed primarily due to the formation of $CaSiAlN_3$ and presence of AlN phases along with the major alpha-sialon phase. For a sample having 14 wt% AlN phase and 86 wt% $CaSiAlN_3$ phase, Y. Cai et al. have reported a Vickers hardness of 14.4 GPa while Stefan R. Witek et al. have reported a hardness of 12 GPa for hot-pressed AlN ceramics [24,43]. Formation of multiple phases (having lower hardness) along with the gradual increase in grain size of α-sialon phase is thought to have contributed towards the gradual decrease in the hardness.

Vickers hardness values in the range of 16-20 GPa and fracture toughness of 3-7 MPa.$m^{1/2}$ has been reported in the literature for the single or multi cation calcium stabilized oxygen rich alpha-sialons [11,22,38,44,45]. In our study, the relatively higher measured hardness may well be attributed to the nitrogen rich alpha-sialons. The observation is line with a study performed by František Lofaj et al. revealing that a 4% increase in N content would result in nearly the same increase in micro-hardness of RE-Si-Mg-O-N systems [46].

4. Conclusion

Calcium stabilized nitrogen rich sialon having compositions along the Si_3N_4:1/2Ca_3N_2:3AlN line were synthesized. Enhanced reaction kinetics due to nano/submicron-sized precursors and high heating rates achieved with the aid of non-conventional SPS process allowed the preparation of well densified nitrogen rich sialon ceramics at relatively low temperature (1500°C as compared to 1700°C or 1800°C). Alpha sialon-phase for samples having Ca content (c) in the range of $0.15 < x < 1.83$ was obtained. Formation of single phase nitrogen rich alpha-sialons was achieved for samples having nominal x value in the range of $0.4 < x < 1.6$. Increase in the lattice parameters of alpha-sialon unit cell was observed to have a linear relationship with the amount of Ca^{+2} ions incorporated in the alpha structure. Increasing x value resulted in an increase in the average grain size from 286nm to 468nm.

Moreover, higher amount of Ca_3N_2 starting powder was observed to facilitate the formation of elongated alpha-sialon grains. Calcium stabilized nitrogen rich sialon ceramics having very promising hardness and fracture toughness of 22.4 GPa and 6.1 MPa.$m^{1/2}$ respectively were developed. Furthermore, the absence of a glassy grain boundary phase in nitrogen rich sialons make them potentially viable candidates for

high temperature applications. It is believed that such engineering ceramic materials would appeal to the industry owing to their unique properties and relatively low processing temperature.

Declarations

Acknowledgement

The authors would like to acknowledge the support provided by King Fahd University of Petroleum and Minerals, Saudi Arabia, and that of the University of Sharjah, UAE.

Compliance with Ethical Standards

Conflict of Interest: The authors declare that they have no conflict of interest.

References

[1] W.-Y. Sun, T.-Y. Tien, T.-S. Yen, Subsolidus Phase Relationships in Part of the System Si,Al,Y/N,O: The System Si_3N_4AlNYN$Al_2O_3Y_2O_3$, J. Am. Ceram. Soc. 74 (1991) 2753–2758.

[2] R.-J. Xie, N. Hirosaki, K. Sakuma, Y. Yamamoto, M. Mitomo, Eu^{2+}-doped Ca-α-SiAlON: A yellow phosphor for white light-emitting diodes, Appl. Phys. Lett. 84 (2004) 5404–5406.

[3] J. Grins, S. Esmaeilzadeh, Z. Shen, Structures of Filled α-Si_3N_4-Type $Ca_{0.27}La_{0.03}Si_{11.38}$ $Al_{0.62}N_{16}$ and $LiSi_9Al_3O_2N_{14}$, J. Am. Ceram. Soc. 86 (2003) 727–30.

[4] S. Suzuki, T. Nasu, S. Hayama, M. Ozawa, Mechanical and thermal properties of beta'-sialon prepared by a slip casting method, J. Am. Ceram. Soc. 79 (1996) 1685–1688.

[5] F. Izumi, M. Mitomo, Y. Bando, Rietveld refinements for calcium and yttrium containing α-sialons, J. Mater. Sci. 19 (1984) 3115–3120.

[6] M.J. Pomeroy, C. Mulcahy, S. Hampshire, Independent effects of nitrogen substitution for oxygen and yttrium substitution for magnesium on the properties of Mg-Y-Si-Al-O-N Glasses, J. Am. Ceram. Soc. 86 (2003) 458–464.

[7] V.A. Gunchenko, V.N. Pavlikov, G. V. Trunov, Kinetics and mechanism of oxidation of β-sialons, Sov. Powder Metall. Met. Ceram. 27 (1988) 470–474.

[8] J. Persson, T. Ekström, P.O. Käll, M. Nygren, Oxidation behaviour and mechanical properties of β- and mixed α-β-sialons sintered with additions of $Y_2O_3$and Nd_2O_3, J. Eur. Ceram. Soc. 11 (1993) 363–373.

[9] L. Liu, R.-J. Xie, N. Hirosaki, T. Takeda, C. Zhang, J. Li, X. Sun, Photoluminescence properties of β-SiAlON:Yb^{2+}, a novel green-emitting phosphor for white light-emitting diodes, Sci. Technol. Adv. Mater. 12 (2011) 034404.

[10] P.L. Wang, C. Zhang, W.Y. Sun, D.S. Yan, Characteristics of Ca-α-sialon—Phase formation, microstructure and mechanical properties, J. Eur. Ceram. Soc. 19 (1999) 553–560.

[11] J.W.T. van Rutten, H.T. Hintzen, R. Metselaar, Phase formation of Ca-α-sialon by reaction sintering, J. Eur. Ceram. Soc. 16 (1996) 995–999.

[12] F.L. Riley, Silicon Nitride and Related Materials, J. Am. Ceram. Soc. 83 (2004) 245–265.

[13] S. Hampshire, H.K. Park, D.P. Thompson, K.H. Jack, α'-Sialon ceramics, Nature. 274 (1978) 880–882.

[14] Z.-K. Huang, P. Greil, G. Petzow, Formation of alpha-Si_3N_4 solid solutions in the system Si_3N_4-A1N-Y_2O_3, J. Am. Ceram. Soc. 66 (1983) C–96–C–97.

[15] Z.-K. Huang, T.-Y. Tien, T.-S. Yen, Subsolidus phase relationships in Si_3N_4-AlN-rare-earth oxide systems, J. Am. Ceram. Soc. 69 (1986) C–241–C–242.

[16] S.-F. Kuang, Z.-K. Huang, W.-Y. Sun, T.-S. Yen, Phase relationships in the Li_2O-Si_3N_4-AlN system and the formation of lithium-α-sialon, J. Mater. Sci. Lett. 9 (1990) 72–74.

[17] Z.-K. Huang, W.-Y. Sun, D.-S. Yan, Phase relations of the Si_3N_4-AlN-CaO system, J. Mater. Sci. Lett. 4 (1985) 255–259.

[18] M. Herrmann, S. Kurama, H. Mandal, Investigation of the phase composition and stability of the α-SiAlONs by the Rietveld method, J. Eur. Ceram. Soc. 22 (2002) 2997–3005.

[19] S.K.M.H. H.Mandal, The effect of processing conditions, amount of additives and composition on the microstructures and mechanical properties of α-SiAlON ceramics, J. Eur. Ceram. Soc. 22 (2002) 109–119.

[20] T.-S. Sheu, Microstructure and Mechanical properties of the in situ beta-si_3n_4/alpha'-sialon composite, J. Am. Ceram. Soc. 77 (1994) 2345–2353.

[21] T. Ekstrom, M. Nygren, SiAlON Ceramics, J. Am. Ceram. Soc. 75 (1992) 259–276.

[22] H. Mandal, D.P. Thompson, α→β Sialon transformation in calcium-containing α-sialon ceramics, J. Eur. Ceram. Soc. 19 (1999) 543–552.

[23] Y.B. Xie, Rong-Jun, Mamoru Mitomo, F. F. Xu, Preparation of Ca-α-sialon ceramics with compositions along the Si_3N_4-1/2 Ca_3N_2:3AlN line, Z. Met. 92 (2001) 931–936.

[24] Y. Cai, Synthesis and characterization of nitrogen-rich calcium [alpha]-sialon ceramics, Department of Physical, Inorganic and Structural Chemistry, Stockholm University, 2009. https://books.google.com.sa/books?id=65ryjwEACAAJ.

[25] C.A. Wood, H. Zhao, Y.-B. Cheng, Microstructural development of calcium alpha-sialon ceramics with elongated grains, J. Am. Ceram. Soc. 82 (2004) 421–428.

[26] F. Ye, M.J. Hoffmann, S. Holzer, Y. Zhou, M. Iwasa, Effect of the amount of additives and post-heat treatment on the microstructure and mechanical properties of Yttrium-α-Sialon Ceramics, J. Am. Ceram. Soc. 86 (2003) 2136–2142.

[27] Z. Shen, H. Peng, M. Nygren, Formation of in-situ reinforced microstructure in α–sialon ceramics I: Stoichiometric oxygen-rich compositions, J. Mater. Res. 17 (2002) 336–342.

[28] Y. Cai, Z. Shen, J. Grins, S. Esmaeilzadeh, T. Höche, Self-Reinforced Nitrogen-rich calcium α-sialon ceramics, J. Am. Ceram. Soc. 90 (2007) 608–613.

[29] Wikipedia contributors, Hot pressing-Wikipedia The Free Encyclopedia, accessed August 16, 2018.

https://en.wikipedia.org/w/index.php?title=Hot_pressing&oldid=827939071.

[30] FCT Systeme GmbH, accessed August 16, 2018.

http://www.fct-systeme.de/en/content/Spark_Plasma_Sinteranlagen/~nm.12~nc.26

[31] R.M.A. Khan, M.M. Al Malki, A.S. Hakeem, M.A. Ehsan, T. Laoui, Development of a single-phase Ca-α-SiAlON ceramic from nanosized precursors using spark plasma sintering, Mater. Sci. Eng. A. 673 (2016) 243–249.

[32] N. Camuşcu, D.P. Thompson, H. Mandal, Effect of starting composition, type of rare earth sintering additive and amount of liquid phase on αa ⇆ β sialon transformation, J. Eur. Ceram. Soc. 17 (1997) 599–613.

[33] B.A. Ahmed, A.S. Hakeem, T. Laoui, R.M.A. Khan, M.M. Al Malki, A. Ul-Hamid, F.A. Khalid, N. Bakhsh, Effect of precursor size on the structure and mechanical properties of calcium-stabilized sialon/cubic boron nitride nanocomposites, J. Alloys Compd. 728 (2017) 836-843.

[34] H.M. Irshad, B.A. Ahmed, M.A. Ehsan, T.I. Khan, T. Laoui, M.R. Yousaf, A. Ibrahim, A.S. Hakeem, Investigation of the structural and mechanical properties of micro-/nano-sized Al_2O_3 and cBN composites prepared by spark plasma sintering, Ceram. Int. 43 (2017) 10645–10653.

[35] M.M. Al Malki, R.M.A. Khan, A.S. Hakeem, S. Hampshire, T. Laoui, Effect of Al metal precursor on the phase formation and mechanical properties of fine-grained SiAlON ceramics prepared by spark plasma sintering, J. Eur. Ceram. Soc. 37 (2017) 1975–1983.

[36] B.A. Ahmed, A.S. Hakeem, T. Laoui, M. Al Malki, M.A. Ehsan, S. Ali, Low-temperature spark plasma sintering of calcium stabilized alpha sialon using nano-size aluminum nitride precursor, Int. J. Refract. Met. Hard Mater. 71 (2018) 301–306.

[37] 12013-82-0 CAS MSDS (calcium nitride) Melting Point Boiling Point Density CAS Chemical Properties, accessed September 24, 2017.

http://www.chemicalbook.com/ChemicalProductProperty_US_CB2672982.aspx

[38] P.L. Wang, C. Zhang, W.Y. Sun, D.S. Yan, Formation behavior of multi-cation α-sialons containing calcium and magnesium, Mater. Lett. 38 (1999) 178–185.

[39] O. Eser, S. Kurama, A comparison of sintering techniques using different particle sized β-SiAlON powders, J. Eur. Ceram. Soc. 32 (2012) 1343–1347.

[40] O. Eser, S. Kurama, The effect of the wet-milling process on sintering temperature and the amount of additive of SiAlON ceramics, Ceram. Int. 36 (2010) 1283–1288.

[41] C.L. Hewett, Y.-B. Cheng, B.C. Muddle, M.B. Trigg, Thermal Stability of Calcium α-sialon Ceramics, J. Eur. Ceram. Soc. 18 (1998) 417–427.

[42] A. Thorel ‴, J.Y. Laval+, D. Broussaud, High temperature mechanical properties and intergranular structure of sialons, Journal de Physique Colloques, 1986, 47 (C1), 353-357.

[43] S.R. Witek, G.A. Miller, M.P. Harmer, Effects of CaO on the strength and toughness of AlN, J. Am. Ceram. Soc. 72 (1989) 469–473.

[44] Z.-H. Xie, M. Hoffman, Y.-B. Cheng, Microstructural tailoring and characterization of a calcium α-sialon composition, J. Am. Ceram. Soc. 85 (2004) 812–818.

[45] Y. Zhang, Y.-B. Cheng, Grain boundary devitrification of Ca α-sialon ceramics and its relation with the fracture toughness, J. Mater. Sci. 38 (2003) 1359–1364.

[46] A. de Lofaj, F; Dorcakova, F; Kovalcik, J; Hoffmann, MJ; Lopez, The effect of lanthanides and nitrogen on microhardness of oxynitride, Kov. Mater. Mater. 41 (2003) 145–157.

Figures

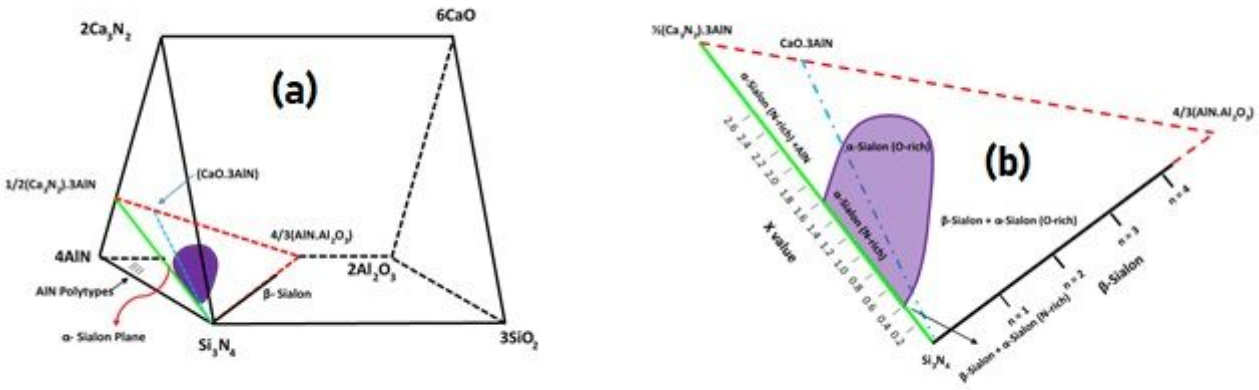

Figure 1

Regenerated schematic representation of (a) Janecke Prism of Ca-sialon system and (b) α-plane in Ca-sialon system at 1800°C [24].

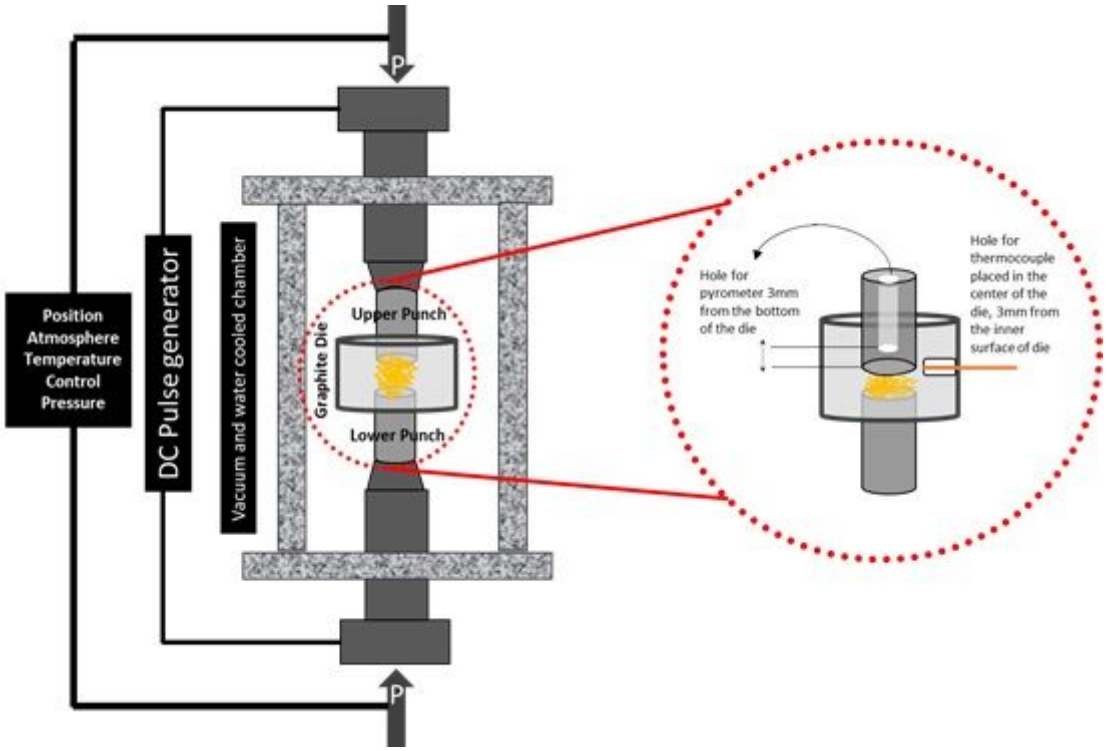

Figure 2

Schematic of spark plasma sintering equipment showing the die and temperature measurement configuration.

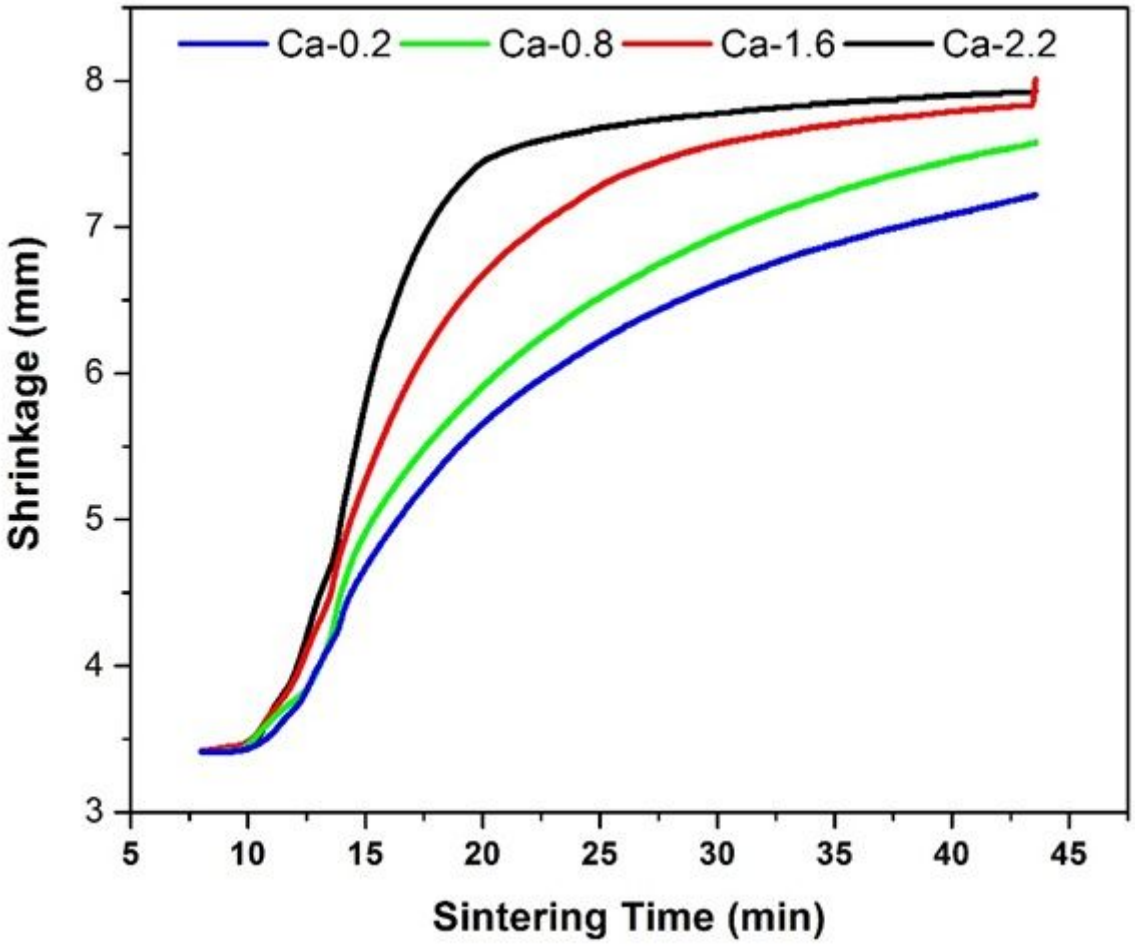

Figure 3

Densification curves of several compositions of calcium stabilized nitrogen rich sialons sintered at 1500°C using spark plasma sintering technique, where Ca content varies between 0.2-2.2. The insert shows the complete densification curves while the main plot represents the selected high temperature region (heating from 1050°C to 1500°C followed by 30 min holding time).

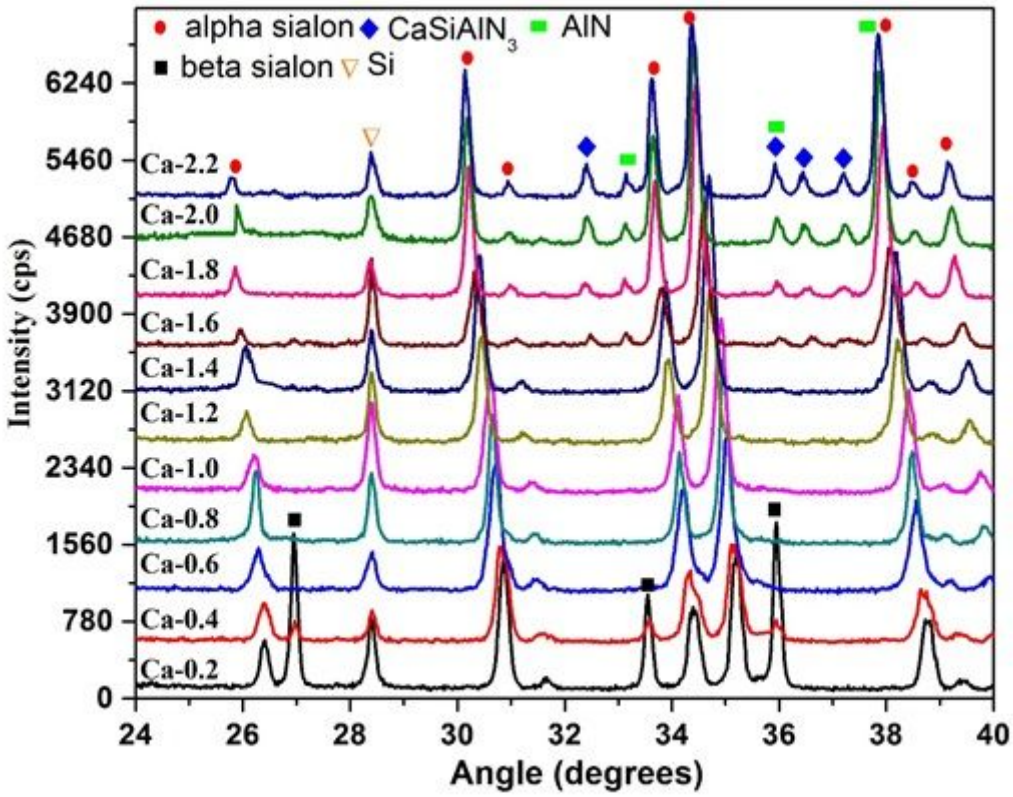

Figure 4

X-ray diffraction patterns of the calcium stabilized nitrogen rich alpha-sialon samples synthesized along the Si3N4:1/2Ca3N2:3AlN line at sintering temperature of 1500□C.

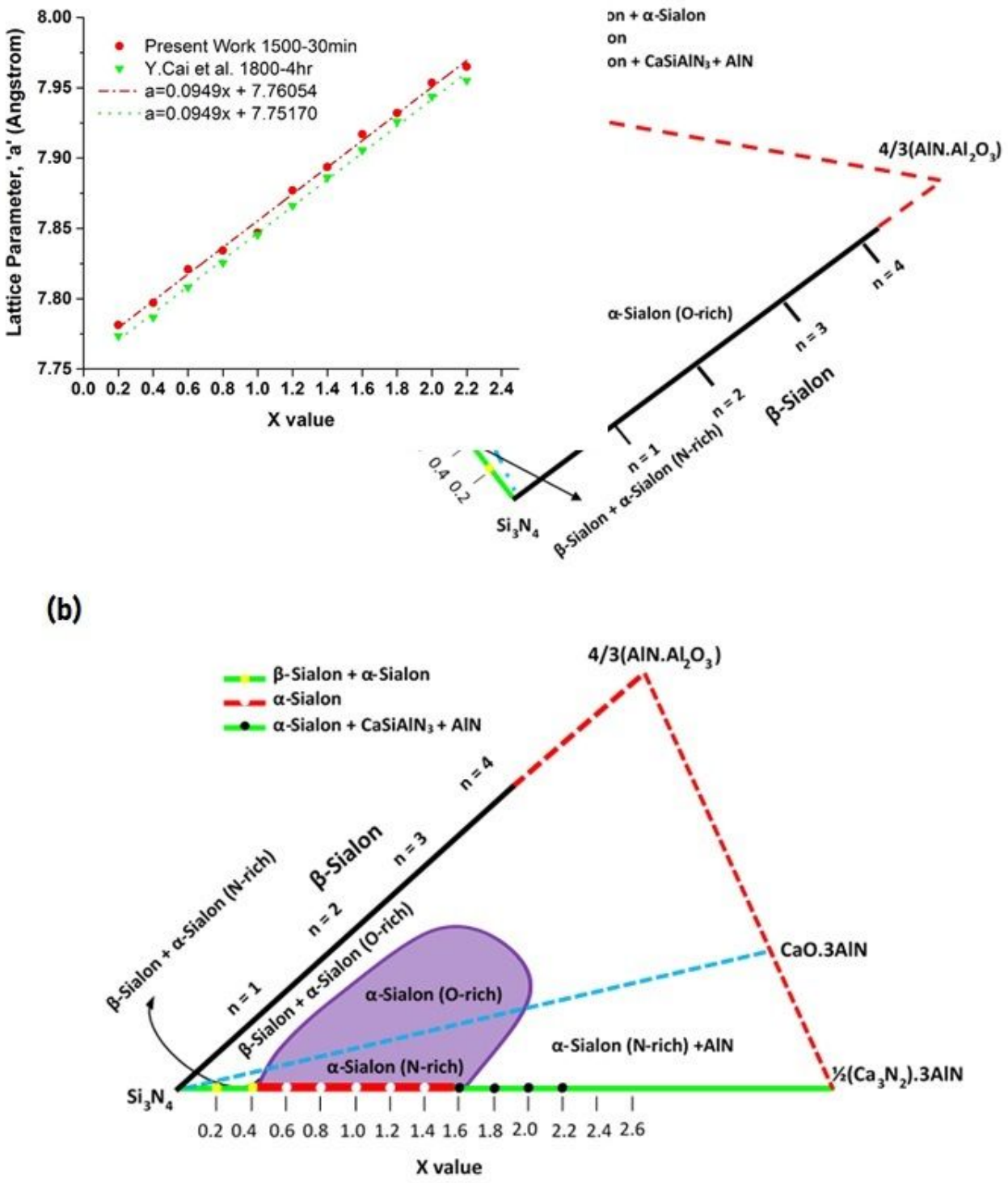

Figure 5

(a) Regenerated schematic representation of α-plane in Ca-sialon system showing phase stability regime along the N'Rich line at 1500°C and (b) another representation where the orientation of the alpha plane is one which is most commonly reported in the literature.

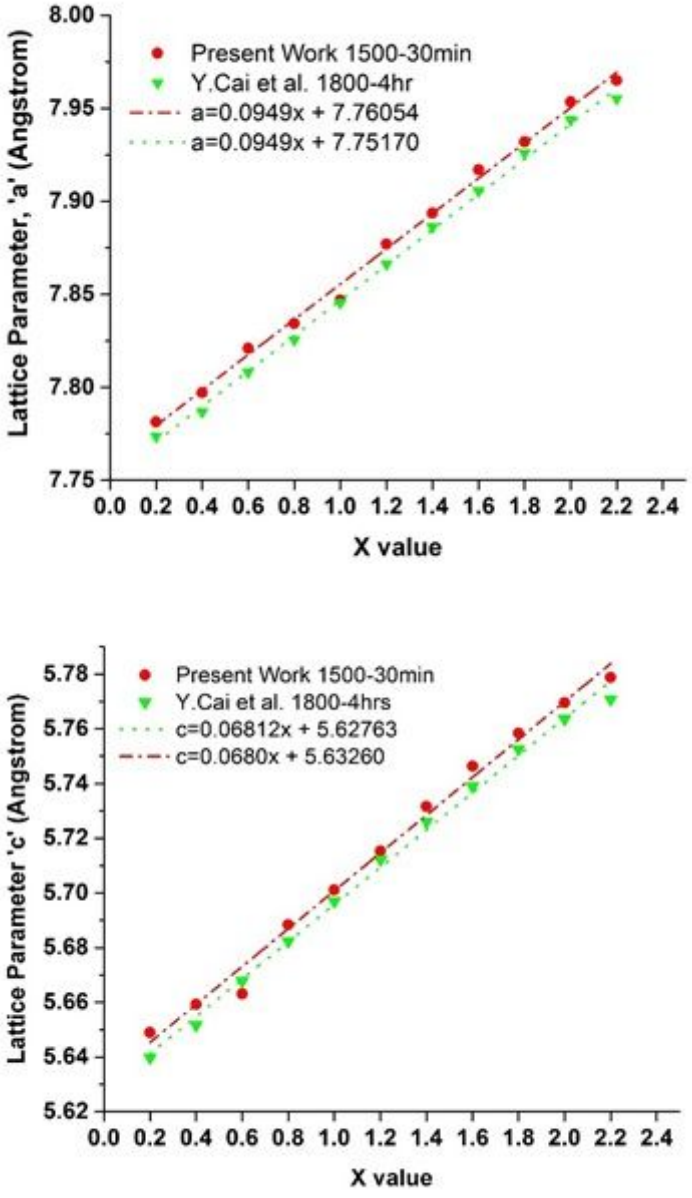

Figure 6

Variation of lattice parameters of calcium stabilized nitrogen rich alpha-sialons with x value for samples synthesized at 1500□C using SPS and those reported by Y.Cai et al. at 1800°C using HP.

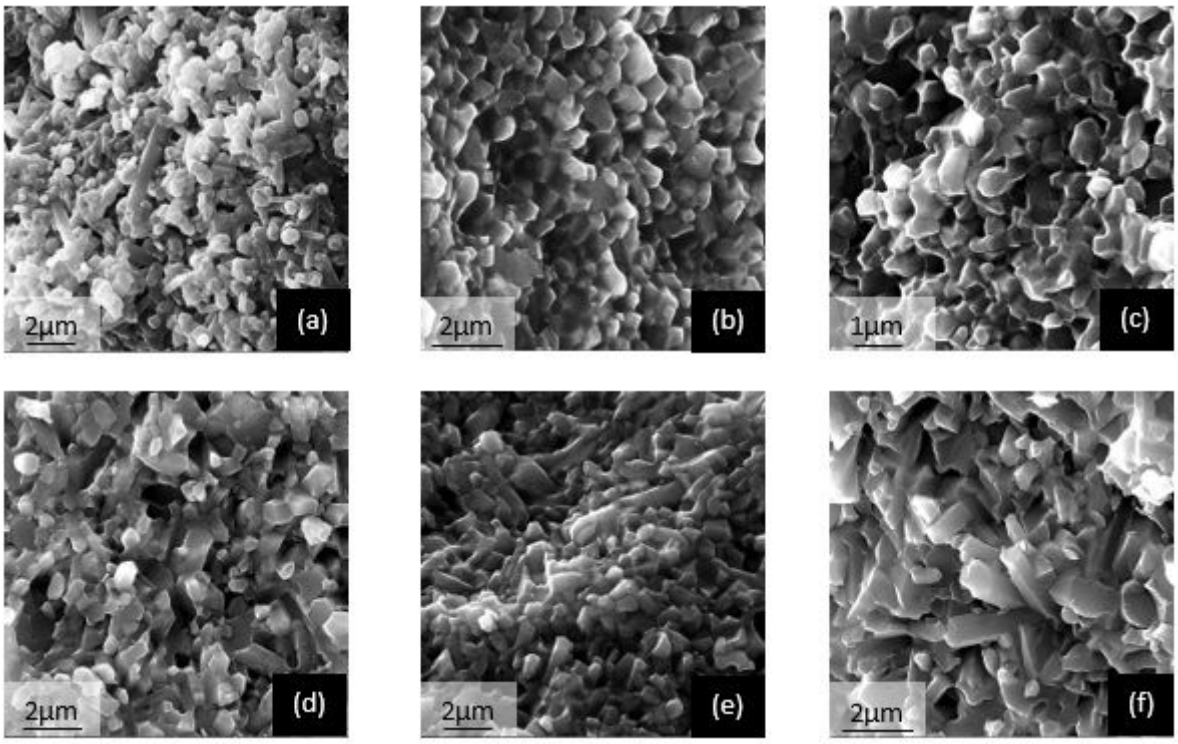

Figure 7

Secondary electron (FESEM) micrographs of the fractured surfaces of nitrogen rich samples synthesized at 1500□C using different x values: (a) Ca-0.2, (b) Ca-0.6, (c) Ca-1.2, (d) Ca-1.6, (e) Ca-1.8 and (f) Ca-2.0.

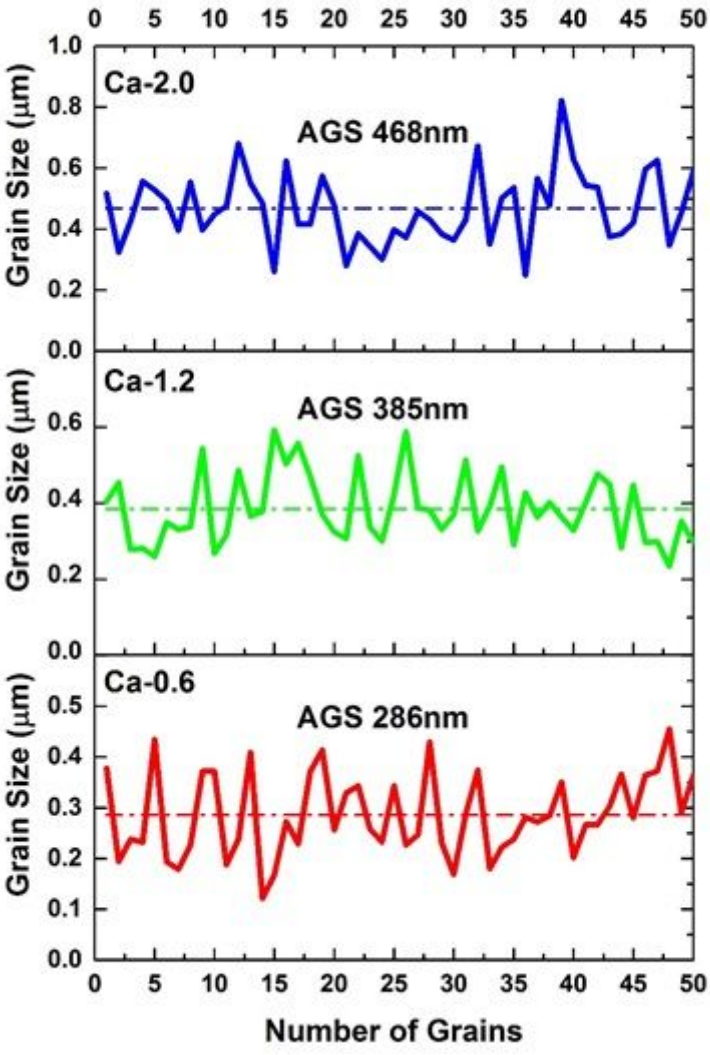

Figure 8

Grain size distribution of nitrogen rich samples synthesized at 1500□C having the sample ID's of Ca-0.6, Ca-1.2 and Ca-2.0.

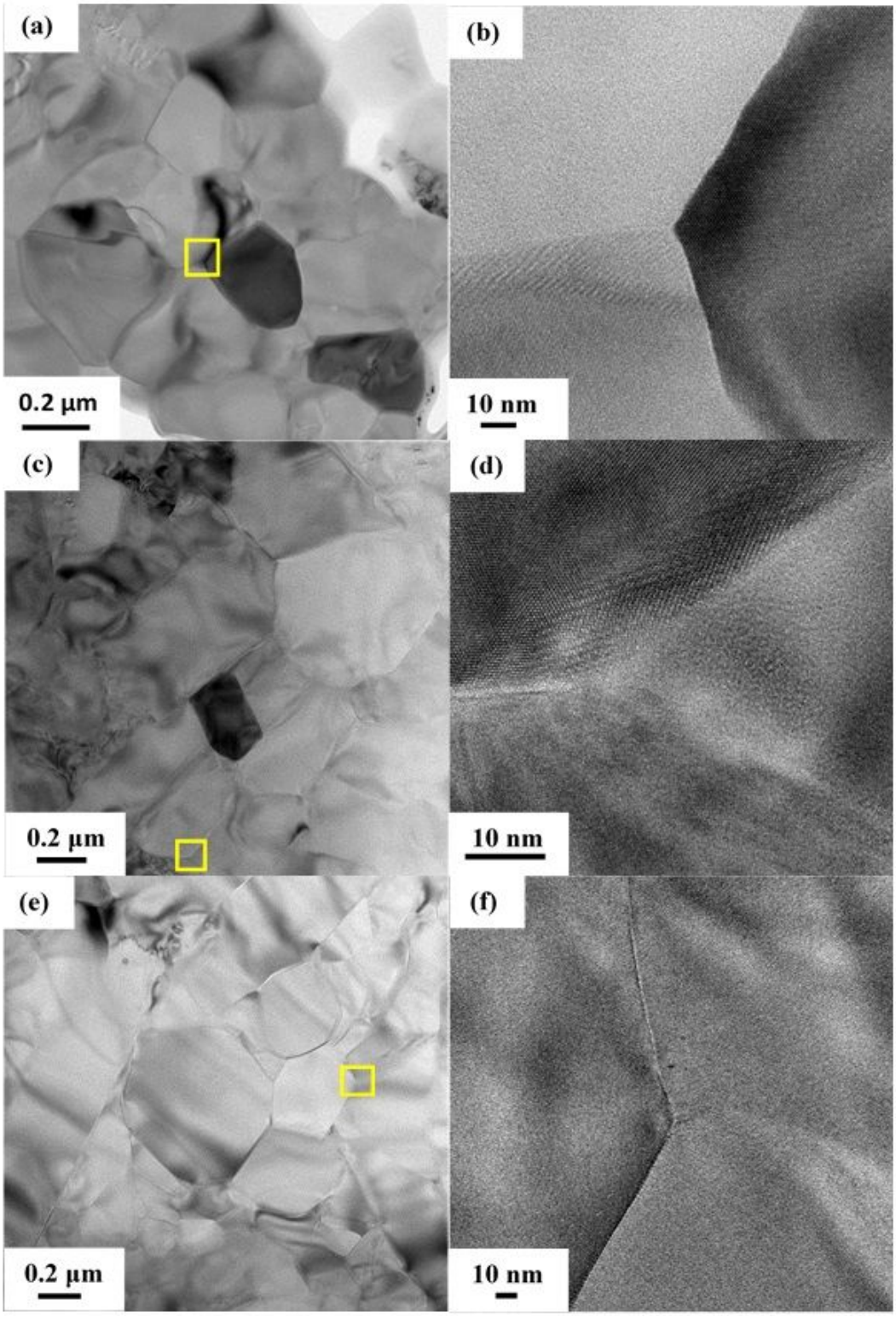

Figure 9

Low and high resolution TEM micrographs of the nitrogen rich samples synthesized at 1500□C using different x values: (a & b) Ca-0.6, (c & d) Ca-1.2 and (e & f) Ca-2.0.

Supplementary Files

This is a list of supplementary files associated with this preprint. Click to download.

- GraphicalAbstract.pdf